Journal of Imaging Science and Technology® 54(5): 050307–050307-6, 2010.

Study of Ink Jet Printing Parameters to Fabricate LCD Color Filter

Seong-Jin Kim, Byung-Hun Kim, Sung-Wook Kim and Seung-Joo Shin
Central R&D Center, Samsung Electro-Mechanics, 314 Maetan3-Dong, Suwon, Gyunggi-Do 443-743, Korea
E-mail: byungh.kim@samsung.com

Alberto Salleo[†], Steve Ready[▲] and Robert Street
Palo Alto Research Center, 3333 Coyote Hill Rd., Palo Alto, California 94304

Abstract. *The ink jet printing technique can be an alternative fabrication route for LCD color filters. The source of luminance nonuniformity in color filters fabricated by ink jet printing is described and methods to minimize this nonuniformity are presented. Both drop volume uniformity of the ink jet printhead and morphology of the printed color filter layer are important to achieve required luminance uniformity. Some practical methods to control the drop volume uniformity were tested and proposed. Morphological control of the printed color filter was also studied. Desirable interfacial energy between color filter and black matrix was modeled and tested using both plasma treatment and solution treatment. © 2010 Society for Imaging Science and Technology.*
[DOI: 10.2352/J.ImagingSci.Technol.2010.54.5.050307]

INTRODUCTION

Ink jet printing technology has been widely used for desktop publication applications. Both thermal bubble jet and piezoelectric impulse ink jet have been commercialized for these applications. The principles of both techniques are well explained in the literature.[1,2] Recently, ink jet printing technology has been considered as a direct patterning method because this technique can be a cost effective route compared to the conventional photolithographic process. Kim and McKean demonstrated the patterning of TiO_2 thick film using the ink jet technique.[3] Ink jet printing as an alternative patterning method has been more widely studied lately in the context of important technological applications including flat panel displays, solar cells, and semiconductors.[4–6] The Shimoda group has been active in the development of the ink jet printing process to fabricate organic light-emitting diodes and liquid crystal displays (LCDs).[7,8] In their work, the important process parameters were described for both devices. Their work provided a practical method of controlling key process parameters to achieve commercially acceptable device quality fabricated by the ink jet printing technique. Suk and Kim used ink jet printing to fabricate LCD color filters.[9] They proposed that drop volume uniformity of the ink jet printhead and surface energy control on the black matrix were key process parameters to achieve *Mura*-free quality.

Mura is a Japanese term meaning unevenness and inconstancy in physical matter. One important quality required for a LCD is to prevent luminance nonuniformity as perceived by the human eye. The source of *Mura* was analyzed by Mori et al.[10] Luminance nonuniformity of the color filter is an important source of *Mura* in LCD panels. Unlike conventional photolithography, ink jet printing may generate thickness and morphological nonuniformity of the color filter layer. These two nonuniformities can be the source of luminance nonuniformity unless controlled within the human perceptual level. The thickness nonuniformity occurs due to a nonuniform amount of liquid ejected from each nozzle of a printhead. The drop volume uniformity of most commercially available printheads is insufficient to produce a color filter panel with the required luminance uniformity. Nonuniform morphology of the color filter layer can occur due to the pinning of the drop edge followed by mass transport of solid ink materials to the edge during drying. This transport is controlled by the local partial pressure distribution over the top of the drop.[11] Another important source of luminance nonuniformity is the microflow of liquids of different color between pixels. This generates undesirable color mixing and is easily perceived by the human eye. The source of the microflow of liquids of different color is described by Kiguchi.[7] A patterned organic bank structure on top of opaque metal, often called the black matrix, is proposed to confine a liquid droplet ejected from the printhead. The surface of the bank was further treated by plasma to enhance liquid-repellent property. It was proposed that such surface treatment is required to prevent undesirable color mixing between the pixels.

In this article, we have tested various methods to control the key process parameters. In order to control drop volume uniformity, some practical control methods are described. The comparison of these methods was performed and their characteristics are described. A method of using drops from different nozzles to achieve the thickness uniformity of the color filter panel is also described. Various meth-

▲IS&T Member.
†Present address: Stanford University, Palo Alto, California 94304.

Received Dec. 18, 2009; accepted for publication Jun. 11, 2010; published online Aug. 3, 2010.
1062-3701/2010/54(5)/050307/6/$20.00.

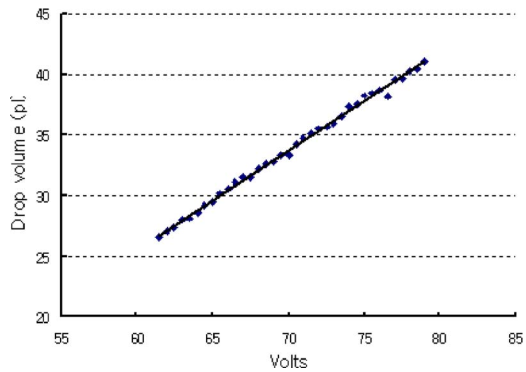

Figure 1. The relation between voltage amplitude of the trapezoidal waveform and the drop volume with Dimatix SE 128.

ods to control the surface energy of the organic black matrix were tested to prevent the intermixing of liquids of different color. The effect of the black matrix structure was studied to understand the spreading process of ink on the glass substrate.

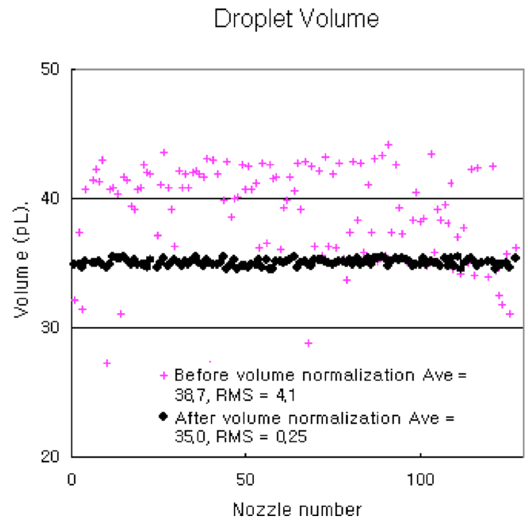

Figure 2. The drop volume variations along the nozzles before and after volume normalization with jetting frequency=1 kHz.

DROP VOLUME CONTROL METHODS

Three different methods to control the drop volume have been explored. First, the drop volume in flight was measured using machine vision, e.g., a charge coupled device (CCD) camera in a stroboscopic setup. While the drops are being fired, the drop volume is measured at a particular nozzle of interest and the waveform is adjusted iteratively *in situ* to obtain the desired drop volume. Prior to the normalization process, the relation between the drop volume and the amplitude of the voltage of the voltage waveform, which mostly determines the drop volume, is obtained, as shown in Figure 1. The normalization is performed by adjusting the waveform voltage for each ejector based on the measured drop size. Because the drop volume is evaluated by the drop images taken with a synchronized light emitting diode (LED) light, accurate drop volume estimation is mostly dependent on the quality of the drop images which has an exposure time of approximately 20–30 ms for a typical CCD camera. If the drop firing frequency is set to 1 kHz, for example, then the one CCD image frame contains the 20–30 drops overlapped at the same position. However, inconsistent drop formation causes undesirable qualities in the drop images such as blurred drop edges which result in estimation of drop volume far off from the real value. The drop volume variation of 128 nozzles after normalization, shown in Figure 2, is dominated by the measurement uncertainty on the drop size.

In Fig. 2 the volume target is 35 ± 0.5 pL with the volume measurement uncertainty of ±0.25 pL when the drop velocity is less than 6 m/s. The resolution of the pixel depends on the magnification of the CCD images, and in the study it was 0.37 μm/pixel. In the process of the drop volume normalization as shown in Fig. 2 the drop velocity variation also reduces from $V_{\rm rms}=0.79$ m/s to $V_{\rm rms}=0.25$ m/s. The average drop velocity was 2.7 and 2.0 m/s before and after normalization, respectively. It is interesting to see that the root-mean-square (rms) estimate of drop volume drops a factor of approximately 16.4, while the rms of drop velocity falls by only about 3.2, which implies that adjusting the waveform amplitude affects the drop volume and velocity; however, the effect of the voltage amplitude change on the drop volume and velocity is different from nozzle to nozzle.

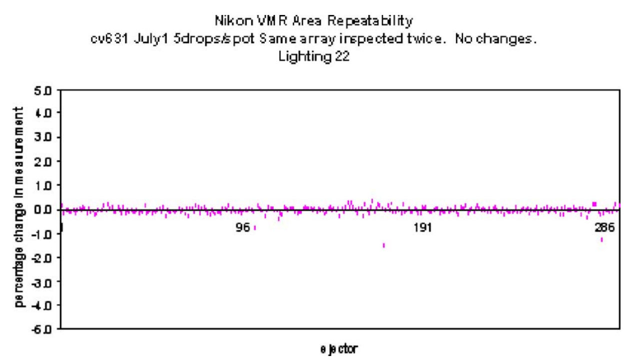

Figure 3. The difference between repeated measurements along the nozzles with the proper light setting on the Nikon VMR.

The second approach is to measure the drop size from the printed spot size on a substrate. An expected advantage of scanning the spot size on a substrate would be to calibrate the printhead more quickly. Several drops are fired from all nozzles onto glass or coated glossy paper substrates with several waveform voltage amplitudes. Then the size of the drop spots are scanned and inspected under a Nikon microscope using VMR light for consistent measurement readings. In order to measure spot size consistently, the illumination light setting needs to be tuned well. The average drop area was obtained by several printed samples and right normalization amplitude of the waveform was evaluated. Similarly, the normalization waveforms corresponding to individual nozzles are determined based on the drop size measurement.

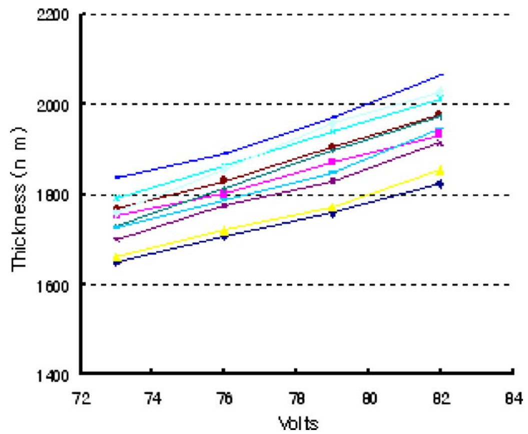

Figure 4. The relation between the voltage amplitude of the trapezoidal waveform and the thickness of the ink for ten nozzles.

Figure 3 shows the unrepeatability of area estimation to be much less than $\pm 0.5\%$ for most of the nozzles, which is much more accurate than the normalization performed with the drop size measurements.

Third, using the thickness of ink deposited on the black matrix (BM) substrate we can normalize the drop volume along the nozzles. This method is similar to the second approach, except drops are printed on the BM substrate and the thickness of the ink is taken into account in the measurements. The thickness of the drop fired onto the color filter pixels shown in Figure 4 increases more or less linearly with increasing voltage amplitudes of the driving waveform. This method allows the accurate calibration of the printhead.

In the printing process, after the individual drop volume from a nozzle of the print head is carefully fixed, the number of drops and drop spacing are automatically established. The volume variation due to the variation in the black matrix height is almost negligible because of its precise photolithographic manufacturing process. The uniformity of luminance of the color filter layer can be achieved by the variation in drop volume for thickness ranges less than approximately 2%. Thus, the total variation in the drop volumes in a pixel array cannot be greater than this limit.

RANDOMIZATION METHOD

If the drop volume variation is normally distributed and the drop measurement error is ignored, then the average drop volume for each nozzle in a printhead when N drops are fired can be written as

$$d_i = \bar{d}_i \pm \frac{\alpha_i}{\sqrt{N}}, \tag{1}$$

where $\bar{d}_i$ is the expected value and α_i is the deviation of drop volume at ith nozzle in a printhead. If the variation α_i is $3\sigma_i$, where σ is the standard deviation, this expression statistically covers approximately 99.7% range of the possible volume variation jetted from a single nozzle. The volume variation in average drop volume obviously decreases with increasing the number of drops $1/\sqrt{N}$ as shown in the second term in Eq. (1), and the averaged volume d_i becomes close to the mean volume $\bar{d}_i$. However, each nozzle has its own mean $\bar{d}_i$ that could be different from that of other nozzles because of the manufacturing variations and internal crosstalk effects. That is why the normalization process is required. For the color filter application it is possible to fill the pixel array with different nozzles to reduce the thickness variations. If K nozzles take part in filling a pixel with the same number of drops N, the average volume can be defined as

$$d_{ik} = \frac{1}{K} \sum \left(\bar{d}_i \pm \frac{\alpha_i}{\sqrt{N}} \right). \tag{2}$$

If the nozzles have the same volume variation α, then Eq. (2) becomes

$$d_{ik} = \frac{1}{K} \sum \bar{d}_i \pm \frac{\alpha}{\sqrt{NK}}. \tag{3}$$

Now, comparing the averaged volume variation in the other pixels, we find that the averaged volume variation of d_{ik} shown in Eq. (2) reduces further because the mean values are averaged out in the first term. Thus, the printing of an individual pixel using multiple nozzles is also effective to reduce the thickness variation of the pixels.

In order to test the printing randomization scheme described above in which a pixel is filled using a combination of different nozzles, a commercially available printhead, Dimatix SE128 (128 nozzles), was used. An arbitrary number of 12 was selected for the number of drops and in the experiments the 12 drops from 64 nozzles were used to fill 64 BM pixels. The thickness of each pixel was measured and used for the simulation of the printing randomization. The second combination used six drops from one nozzle and six drops from another nozzle, and the third combination used three drops from four different nozzles. The two randomized printings show smaller thickness variation in the range and standard deviation than those with 12 drops from one single nozzle. The results are summarized in Table I. Note that the standard deviation decreases with the factor of $1/\sqrt{K}$ when the printing randomization number K increases. The reason is that the mean volume d_i for each nozzle could be normally distributed along the printhead, and in the simulation the volume variation by drops in the second term in Eq. (3) is ignored because the same thickness profiles were used without any variations. The results demonstrate that print-

Table I. Drop volume uniformity of various printing conditions.

Printing condition	Range (%)	Standard deviation	Normalized printing time
12 drops/nozzle ($K=1$)	7.025	1.405	1
6 drops/nozzle ($K=2$)	3.907	0.994	2.063
3 drops/nozzle ($K=4$)	2.415	0.697	4.188

ing with multiple ejectors into each pixel is an effective means of improving uniformity.

To achieve the target thickness range variation of approximately 2%, the printing randomization is carried out based on the thickness measurement after the initial printing. However, there is a trade-off between the number of the printing steps for the randomization and the target variation of the drop volume normalization. If the drop volume is tightly controlled in the drop volume normalization with a small range volume variation, the number of the randomization printings can be decreased further even to zero, i.e., without randomization. In actual mass production, the printing time is decided by the size of the color filter substrates, the number of printheads, and printing speed. Thus, the multiple printheads are used for the same color to reduce the printing time, and in this article the printing speed is set at approximately 400 mm/s.

SURFACE ENERGY CONTROL OF THE BLACK MATRIX

The color filter is printed from a solution that usually contains about 5% by volume of the color pigment, and the final dried film needs to be 1–2 μm thick. The liquid that is printed into the cell therefore extends far above the typical 2 μm height of the black matrix well structure. The liquid must therefore be contained by the surface energy of the well. The display subpixel is a rectangle, and the confinement of the liquid is determined by the shorter dimension which is the width, W_M, of the well. In order to estimate the minimum surface energy of the black matrix, a model calculation of the printed color filter was performed. We assume a cylindrical shape of color filter element (subpixel) in the black matrix as shown in Figure 5, accordingly, the volume of the printed liquid is related to the contact angle, θ, at the edge of the black matrix, according to the following equation:

$$V_M = \frac{{W_M}^2}{4\sin^2(\theta)} L[\theta - \sin(\theta)\cos(\theta)]. \tag{4}$$

The volume of liquid is related to the thickness, D_F, of the dry film by

$$V_M = W_M L D_F C_P, \quad \text{hence } D_F = \frac{W_M}{4C_P \sin^2(\theta)}[\theta - \sin(\theta)\cos(\theta)], \tag{5}$$

where C_P is the pigment loading of the solution. Equation (5) shows that the required contact angle depends on the width of the subpixel, so that a smaller subpixel must have a larger contact angle. At a sufficiently large subpixel width, Eq. (4) no longer applies because the liquid does not conform to a cylindrical shape.

The required contact angle can be estimated using these equations. Fig. 4 plots the relation in Eq. (4) between the minimum contact angle and the dry film thickness for the specific pixel dimensions used. The color filter ink used in this article showed a color gamut close to 70% of National Television System Committee (NTSC) requirements when its thickness is ~1.5 μm. The required surface energy, then, provides a contact angle of at least 25° for a 1.5 μm thick filter.

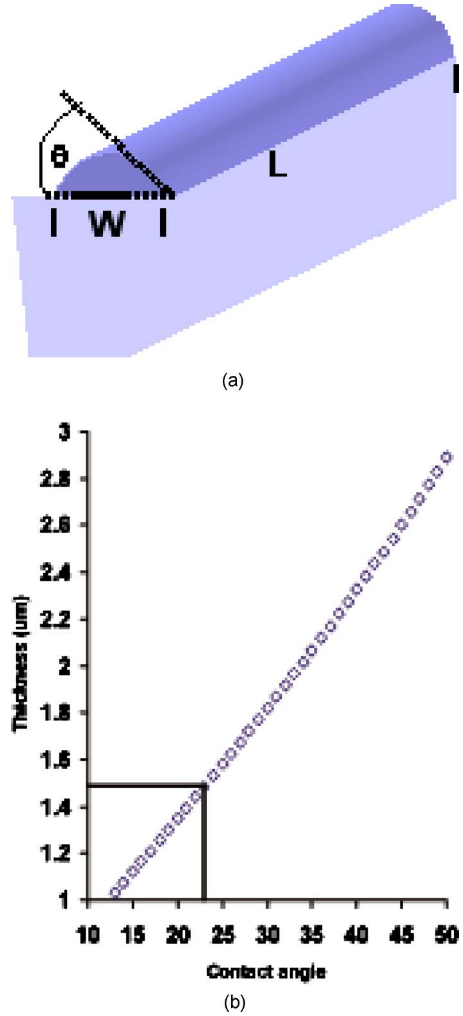

Figure 5. (a) Cylindrical model of the filter ink printed into the black matrix. (b) Plot of maximum thickness of the filter vs the contact angle at the black matrix.

The printing process requires that the well is hydrophilic so that the printed liquid wets the inside of the well uniformly, but the black matrix must be sufficiently hydrophobic to hold the liquid. It is preferable that only the top surface of the black matrix is hydrophobic since otherwise the liquid edge will be pinned at the bottom of the black matrix bank and the thickness of the dried film might decrease at the edge of the subpixel.

Plasma treatment is a well-established technique for surface treatment. The contact angle of dipropylene glycol monomethyl etheracetate (DPMA) on the black matrix surface is ~60° when the matrix is treated with a plasma gas mixture of CF_4/O_2 95%/5%. Figure 6 shows a printed color filter on 10 cm black matrix glass. A 10 cm black matrix on glass, with pixel size 70 μm × 264.5 μm was used. The ink is confined in the black matrix and its thickness is about 1.5 μm, compared to the 2.2 μm height of the black ma-

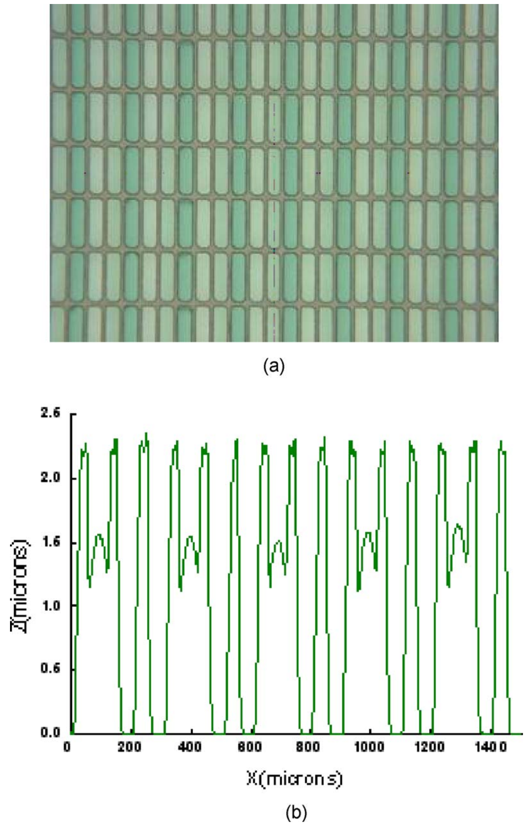

Figure 6. (a) Printed green color filter in black matrix using the CF_4/O_2 method. (b) Thickness profile of color filter material.

trix wall. The figure shows that the dry film is slightly thinner near the black matrix, which we explain by the pinning of the liquid at the bottom of the well.

An alternative surface treatment technique was also studied specifically to make only the top surface of the black matrix hydrophobic and is illustrated in Figure 7. By using a backside exposure and an image reversal step, photoresist is patterned inside the pixel well, leaving the top and part of the sidewalls of the black matrix exposed for chemical treatment with an octadecyltrichlorosilane (OTS) solution. After spin coating (Shipley 1813) or spray coating (Shipley 1513) the photoresist, the substrate is soft baked (5 min at 95°C for S1813; 1 h at 50°C followed by 3 min at 120°C for S1513) and then exposed through the backside of the substrate (30 s at 8 mJ/cm^2). The image reversal process is

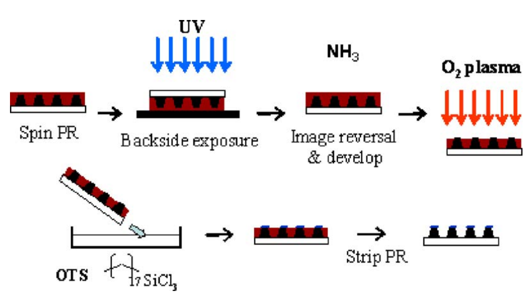

Figure 7. Schematic of image reversal process to make the top of the black matrix well hydrophobic.

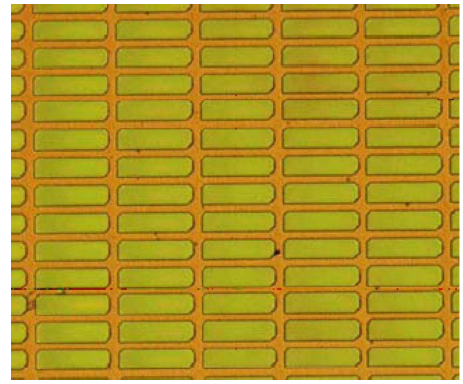

Figure 8. Printed color filter on 10 cm BM glass with image reversal process.

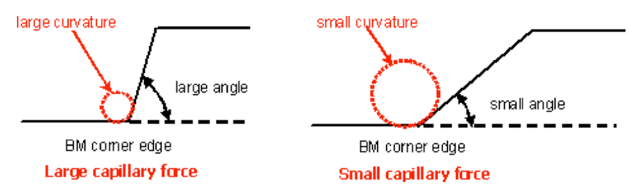

Figure 9. Illustration of the effect of tapering angle on spreading of ink in the black matrix.

carried out in an oven at 95–105°C in an ammonia atmosphere for ~1 h. The substrate is then flood exposed (2 min at 8 mJ/cm^2) and developed (MTF 120 for ~2–5 min). For the OTS part of the process, the substrate is first exposed to an O_2 plasma to activate the surface of the BM, immersed in a 0.2% v/v solution of OTS in hexadecane for 20 min, and rinsed in heptane. The photoresist is then stripped in acetone and the substrate is ready for printing. This method provides a desirable surface as well as a flat color filter profile, but is a more complex process. Figure 8 shows a photograph of a printed green color filter using the image reversal process.

In addition to the surface treatment of black matrix, a numerical analysis was carried out to study how the structure of black matrix influences the filling process of color filter materials in the black matrix. A printing condition was assumed as follows:

(1) Drop volume=20 pL,
(2) Drop velocity=3 m/s,
(3) Viscosity=10 cps,
(4) Surface tension of ink=28 mN/m.

When such ink is dropped at the three types of black matrix corner, i.e., (i) square, (ii) chamfered, and (iii) circular, there was no significant difference in terms of spreading in the black matrix. When the tapering angle is increased, the ink is filled into the black matrix well due to the larger capillary force, as illustrated in Figure 9. We conclude that the black matrix design should focus more on the tapering angle than on the corner shape.

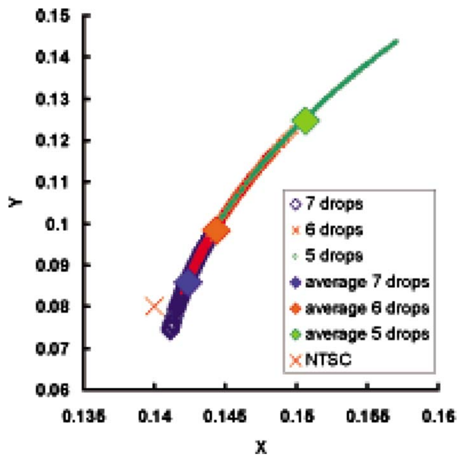

Figure 10. Plot of the color coordinates of ink jet printed blue color filters as a function of the number of drops. The range of values corresponds to measurements from different pixels.

COLOR ACCURACY

The required thickness accuracy and uniformity of the printed color filter depend on the optical absorption spectrum of the filter material and are different for each color. The color coordinates, $C_{X,Y,Z}$, of the CIE plane are given by

$$C(i) = \int S(\lambda)T(\lambda)M(\lambda,i)d\lambda, \qquad (6)$$

where $T(\lambda)$ is the optical transmission, $M(\lambda)$ is the known color matching function, $S(\lambda)$ is the lamp spectrum, and the index i corresponds to red, green, and blue filters. The transmission spectrum can be calculated from $T(\lambda)=e^{-\alpha(\lambda).Z}$, where $\alpha(\lambda)$ is the absorption coefficient of the color filter film and Z is the film thickness. The absorption coefficient was measured in a spin-cast thin film of the same color filter material.

Thickness variations change the color coordinates along a trajectory in (X,Y) space. For the red filter, a thickness variation causes a change in the X coordinate but very little change in the Y coordinate. In contrast, the green filter is more sensitive to thickness variation and both X and Y coordinates are affected.

The effect of the filter thickness on the color coordinates was studied based on Eq. (6). Figure 10 shows the measured color coordinates for a printed blue filter, with different numbers of printed drops, using a single ejector. The NTSC blue coordinate is approached as the number of drops increases from 5 to 7, and Fig. 10 shows the color coordinate trajectory as thickness is varied. The range of values corresponds to measurements of different pixels for a specific printing condition. The data for seven printed drops show a range of about ± 0.01 in the Y coordinate and a considerably smaller variation in the X coordinate.

SUMMARY

Key process parameters for application of ink jet printing to LCD color filter fabrication have been described. Three techniques to control the drop volume from printhead nozzles were proposed in this article. The conventional method using machine vision with a CCD camera in a stroboscopic setup was not accurate enough to produce desirable drop volume uniformity. When this technique was used, the luminance nonuniformity of the printed color filter panel was perceivable by the human eye. An alternative method based on the measured thickness of printed color filter materials was sufficiently accurate to produce luminance uniformity.

Another important parameter is interfacial energy control between color filter ink and the black matrix. Both CF_4/O_2 plasma treatment and OTS coating were effective at preventing ink flow to adjacent pixels. CF_4/O_2 treatment, however, provided ink-repelling property on both top and sidewall surfaces of the black matrix. However, OTS coating provided ink-repelling property only on the top of the black matrix; thus plasma treatment may produce a convex color filter morphology. The effect of morphology on luminance uniformity needs further study. The black matrix tapering angle influences the spreading of ink in the pixel. It was found that a larger tapering angle is desirable. Practical process parameters were defined and tested in this study. This work is expected to help in designing the ink jet printing process for fabrication of other large area devices.

Currently the luminance uniformity target has been achieved by drop volume normalization and printing randomization processes. However, to increase the process yield to the yield of conventional photolithography, studies related to improving the jetting stability of ink jet print heads and on the inspection techniques for large size of printed color filter substrates are required in the future.

REFERENCES

[1] R. C. Durbeck and S. Sherr, *Output Hardcopy Devices* (Academic Press, New York, 1988).

[2] D. B. Bogy and F. E. Talke, “Experimental and theoretical study of wave propagation in drop-on-demand ink jet devices”, IBM J. Res. Dev. **28**, 314–321 (1984).

[3] S. J. Kim and D. E. McKean, “Aqueous TiO_2 suspension preparation and novel application of ink-jet printing technique for ceramic patterning”, J. Mater. Sci. Lett. **17**, 11 (1998).

[4] S. E. Ready, W. S. Wong, A. Arias, R. B. Apte, M. L. Chabinyc, and R. A. Street, “Toolset for printed electronics”, *Proc. IS&T's Digital Fabrication 2006* (IS&T, Springfield, VA, 2006).

[5] S. R. Forrest, “The path to ubiquitous and low-cost organic electronic application on plastics”, Nature (London) **428**, 911–918 (2004).

[6] B. de Gans, P. C. Duineveld, and U. S. Schubert, “Ink jet printing of polymers: State of the art and future development”, Adv. Mater. **16**, 203–213 (2004).

[7] Hiroshi Kiguchi, “The current situation and future application of ink jet industry”, *Proc. IS&T's Digital Fabrication 2005* (IS&T, Springfield, VA, 2005) pp. 113–118.

[8] T. Shimoda, K. Morii, S. Seki, and H. Kiguchi, “Ink jet printing of light emitting polymer displays”, MRS Bull. **28**, 821–827 (2003).

[9] Jun H. Souk and Byong Joo Kim, “Ink jet technology for large size color filter plate”, SID '08 Digest **37**, 429–432 (2008).

[10] Y. Mori, K. Tanahashi, and S. Tsuji, “Quantitative evaluation of “mura” in liquid crystal displays”, Opt. Eng. **43**, 2696–2700 (2004).

[11] R. D. Deegan, O. Bakajin, T. F. Dupont, G. Huber, S. R. Nagel, and T. A. Witten, “Capillary flow as the cause of ring stains from dried liquid drops”, Nature (London) **389**, 827–829 (1997).